The relationship between Soliton and Seismic Wave and the center of 2011 TOHOKU Great Earthquake.(Science of form)

*Masaru Nishizawa[1]

1.none

1. Preface : We had feeled two strong earthquake north of Fukusima Prefecture in the earthquake of 2011 the TOHOKU District Pacific Ocean Earthquake.
In this paper, in this second strong earthquake, the soliton was occurred. (Fig.-1) Still more the second strong earthquake was occurred along the axis of the Japan trench. I could proved two methods.
2. The relationship between Soliton and the center of this earthquake.
At K-NET Oshika (MYG011)(Fig.-1), the epicenter length is 121km. This center is first earthquake motion in seismic wave.
Depend on reference (2), Slip Progression in terms of ship amount is spreading off the coast of MIYAGI Prefecture and is spreading to the north part direction along the axis of the Japan trench after 50 seconds. After 60 secs~100secs, large slip is spreading off the coast from the southern part IWATE prefecture to the north part of FUKUSHIMA prefecture along the axis of the Japan trench. (Fig-4 in reference (2))
In this reference, the total moment rate function (fig-5 in reference (2)) showes Soliton. It is as clear as day. (refer to Fig.-1)
This peak point happened before and after the 80 sec of Seismic moment rate. Therefore this reference showes the second earthquake motion along the axis of the Japan trench.
3. Relationship between Soliton and still more location of the second strong earthquake motion and Seismic Wave.
At K-NET Tsukidate (YYG004) or K-NET Oshika (MYG011), strong-motion accelerograms continues for two earthquake motions in Seismic Wave. In short, the first seismic wave peak and the second seismic wave peak quaked continuous motion. Two strong motion with a small continuous shocks of an earthquake in between exist. For that reason, the second earthquake motion had happened off the coast of the first earthquake motion.
Abstract
1. Strong-motion accelerograms recorded at K-NET Tsukidate (MYG004) or Oshika (MYG011 and others) express clearly a continuation of two earthquake motion.
Therefore the second earthquake motion had happened off the coast of the first earthquake motion. And still more the second earthquake motion was occurred along the axis of the Japan trench. It is an earthquake directly above its epicenter. That’s perfectly right.
2. the total moment rate function (Fig.-5 in reference (2)) shows Soliton.
Reference
1) Sekiguchi, H., Irikura, K., and Iwata, T. (2000): Fault geometry at the rupture termination of the 1995 Hyogo-ken Nanbu earthquake. Bull. Seismol. Soc. Am., 90-1, 117-133, doi: 10.1785/0119990027
2) Wataru SUZUKI, Shin AOI, Haruko SEKIGUCHI, and Takashi KUNUGI. (2012): Source Rupture Process of the 2011 off the Pacific Coast of Tohoku Earthquake Derived from Strong-Motion Records. Bull. Research Report on the 2011 Great East Japan Earthquake Disaster.: March 2012, Natural Disaster Report No. 48: National Research Institute for Earth Science and Disaster Prevention, Japan.
3) Masaru Nishizawa. (2013): The Relationship between in GPS wave gage and Seismic Wave of 2011 the Tohoku District Pacific Ocean Earthquake.: May 19-24 2013 JpGU

Keywords: 2011 the TOHOKU District pacific Ocean Earthquake, Two strong earthquake motion, Soliton, Total moment rate, Science of Form

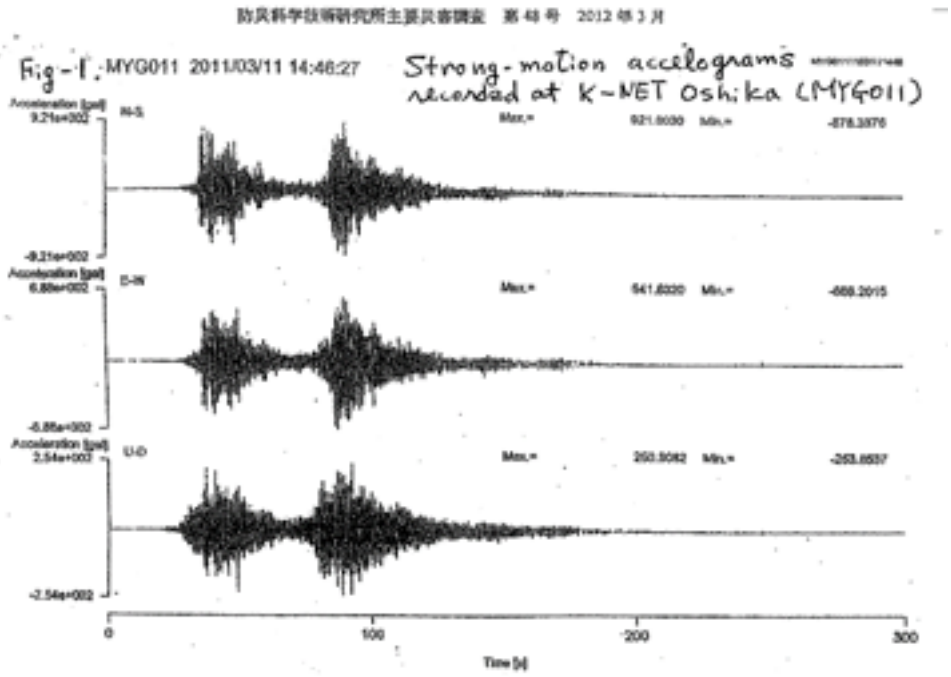

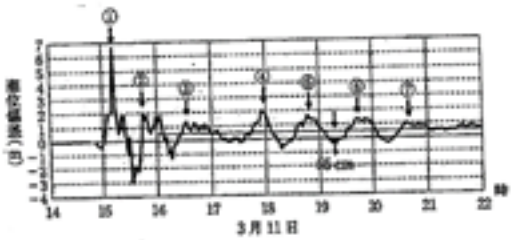

Soliton ① is recognized in GPS wave gage of 2011 the ToHoku District pacific.

Written by Kazuo Oike.

「Great Earthquak of the Japan Ilands」 Iwanami Science Library -185, P10.

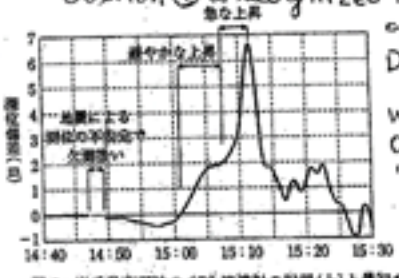

図2 岩手県南部沖のGPS波浪計の記録(上)と最初の部分の拡大図(下)。国土交通省のデータをもとに作成

○ 尾池和夫著「日本列島の巨大地震」岩波科学ライブラリー185, P10.

① ~ Soliton ② ~ ⑦ : Break down of Solitary Wave Solitons.

Reference
「Hydrodynamics」
Written by Mikio Hino. Asakura publisher. 1992

参考：日野幹雄著「流体力学」朝倉書店. 1992

Design and Implementation of the National Seismic Monitoring Network in the Kingdom of Bhutan

*Shiro Ohmi[1], Hiroshi Inoue[2], Jamyang Chophel[3], Kinley Namgay[3], Dowchu Drukpa[3]

1.Earthquake Hazards Division, Disaster Prevention Research Institute, Kyoto University, 2.National Research Institute for Earth Science and Disaster Prevention , 3.Department of Geology and Mines, Ministry of Economic Affairs, Kingdom of Bhutan

Bhutan-Himalayan district is located along the plate collision zone between Indian and Eurasian plates, which is one of the most seismically active region in the world. Recent earthquakes such as M7.8 Nepal earthquake in April 25, 2015 and M6.7 Imphal, India earthquake in January 3, 2016 are examples of felt earthquakes in Bhutan. However, there is no seismic monitoring system established in Bhutan, whose territory is in the center of the Bhutan-Himalayan region.
In this project, we are establishing the first national permanent seismic monitoring network in the Kingdom of Bhutan that is utilized for not only for seismic disaster mitigation of the country but also for studying the seismotectonics in the Bhutan-Himalayan region which is not precisely revealed due to the lack of observation data in the past.
We started establishing permanent seismic monitoring network of minimum requirements which is composed of six (6) observation stations in Bhutan with short period high sensitivity and strong motion seismometers as well as three (3) broad-band seismometers. Obtained data are transmitted to the central processing computers in the DGM (Department of Geology and Mines, Ministry of Economic Affairs) office in Thimphu. In this project, DGM will construct seismic vault with their own budget which is approved as the World Bank project and Japan team assists the DGM for site survey of candidate observation site, designing the observation vault, and designing the data telemetry system as well as providing instruments for the observation such as seismometers and data recorders.
We already started the operation of the first telemetry seismic station located in Thimphu city, the capital in western Bhutan, and will soon start operation in Bumthang district, central Bhutan. Continuous seismic record from Thimphu station is already stored in the data center in DGM. We also deployed two offline seismic stations with short period seismometers in Gasa (Northern Bhutan) and Wangdu (Central) to assist permanent seismic network.

Keywords: Bhutan-Himalayan district, Seismic Observation Network

An improvement of JMA's earthquake catalog

*Satoshi Takahama[1], Koji Tamaribuchi[1], Ken Moriwaki[1], Kana Akiyama[1], Nobuyuki Hirota[1], Naoyuki Yamada[1], Masaki Nakamura[1], Tetsuo Hashimoto[1]

1.Japan Meteorological Agency

Based on the policy of the Headquarters for Earthquake Research Promotion, Japan Meteorological Agency(JMA) collects the data of the high-sensitive seismographs nationwide, performs the processing of hypocenter determination centrally, and publishes the result as the earthquake catalog.
In the current earthquake catalog, we list earthquakes that are limited by a certain criteria as a result of scrutiny. After the 2011 off the Pacific coast of Tohoku Earthquake, although aftershocks have decreased, seismic activity is located in the active situation in comparison with the previous. So we are processing them to raise the lower limit of the magnitude of earthquakes to be processed. Therefore, there is an earthquake smaller than the processing limit that is not listed in the earthquake catalog even if detected by automatic processing.
Against the background of this thing, under the Earthquake Research Committee, an examination for improvement for the way of earthquake catalog was performed in 2013 fiscal year, and summarized reports that shows three directions, 1) to maintain the earthquake detection capability, 2) to list all of the earthquakes detected to the earthquake catalog, 3) to perform the quality management with a stage to accuracy.
Based on this report, JMA is planning to improve and change the hypocenter determination process, utilizing automatic hypocenter etc. In the next catalog, we will promote efficiency of the work procedure as follows.
We utilize the automatic hypocenters in case of the earthquakes smaller than the limit of the magnitude based on the area and the depth of the hypocenter, and we list the earthquakes almost uniformly scrutinized by hands as before in case of the earthquakes larger than this limit. And if the automatic hypocenter is not determined, we list the earthquakes by hands with the simple method using the data of the max about 10 seismic stations.
The lower limit of the scrutinized earthquakes is about M2 in case of shallow and inland earthquakes. This lower limit increases with distances from the coast of the lands, and the max lower limit is about M4.
And newly we introduce registration flags indicating the difference in processing method and the accuracy of the hypocenter.
Here, we will give the concrete examples of materials JMA made with the new earthquake catalog, such as the seismicity map.

Keywords: earthquake catalog

Compiling the source area data of large earthquakes in the world

*Yuzo Ishikawa[1]

1.The National Institute of Advanced Industrial Science and Technology

The earthquake sources in the world are estimated by the area obtained by the one month aftershock distributions. Most of events of which magnitude are larger than 7.5 from 1970, using mainly PDE earthquake catalog. Some large events in 20 century were added using the intensity distributions.

Keywords: source area, large earthquake

The difference between JMA magnitude and moment magnitude in terms of seismic efficiency

*Kiyohiko Yamamoto

1. Introduction: For large earthquakes occurring along the Japan trench except for the off Miyagi Pref. region, moment magnitude Mw is 0.4 larger than the JMA magnitude Mj. Here, Mj and Mw are proportional to logarithms of seismic energy Es and released moment Mo, respectively. Mo is proportional to the relative displacement ub of fault surfaces. Es depends on directly seismic efficiency f, but Mo does indirectly. Thus the difference is thought to reflect the degree of the dependence on f.
f is a function of the rupture velocity Vr and is large for a large Vr. The small Mj compared with Mw thus suggests the small Vr. The difference between Mj and Mw is discussed from this viewpoint for The Tohoku earthquake (2011/3/11, Mw9) as an example.
2.Theory: The damage zone fault model of earthquakes* is employed for the present discussion. In this model, a fault zone with a uniform thickness constitutes of damaged rock area and asperity area. Fault surfaces mean the boundaries between fault zone and host rock blocks. The damaged rocks have relaxed during a long time after the preceding faulting. An asperity has the same elastic constants as the host rocks. Faulting occurs at the time that the relative displacement ub reaches the critical value.
For faulting, energy balance is written by
Pa+Pb=Es+W, Es=f x Pb. (1)
Here, Pa and Pb respectively are strain energies in the asperity and in the host rock blocks. Pb is approximated by the strain energy released when a circular crack is produced in a homogeneous host rocks under the uniform stress, that is equal in magnitude to the average stress drop due to faulting.
W is apparent fracture energy that is equivalent to the work to the host rocks done by the vertical displacement of the fault surfaces. The displacement is produced by the rotation of damaged rocks accompanied by the rupture propagation in a fault zone.
A linear relation has been found between the width of fault damage zone and the length of fault (Vermilye, J. M., and C. H. Scholz, 1998). In order to link the model to fault size, the linear relation is adopted.* Further, Sato and Hirasawa (1973) present an approximate relationship between Vr and f for a circular crack. This relationship is used for the present discussion.
3. Results: For f=1, all strain energy Pb is dissipated as Es. The fraction of asperity area is about 2% of the fault zone area. Vr is approximately equal to the S-wave velocity of host rocks.
For f close to zero, all strain energy Pa+Pb is used for the rupture propagation and Es and Vr go to zeros. These may be the characteristics of so-called slow slip events. The fraction tends to about 0.74%. This is 0.37 times of the fraction at f=1. This means that the displacement and the average stress drop decrease to 0.37 times of those at f=1.
The relationships between Es and Mj and between Mo and Mw respectively are written by
logEs = 1.5M + 4.8 (2)
LogMo = 1.5Mw + 9.1. (3)
For a constant fault area, Eq. (2) and Eq. (3) intersect around f = 0.8. This suggests that the seismic efficiency is about 0.8 for majority of earthquakes. For f = 0.8, Vr is determined at about 0.8 times of S-wave velocity Vs of host rock.
Referring to the report by JMA**, Mj and Mw of The Tohoku earthquake are 8.4 and 9.0, respectively, and Vr and Vs are about 1.8km/s and about 3.4 km/s, respectively. Vr is about 0.53 times of Vs. From the relationship of Vr and f, f is estimated at about 0.3. Mj is estimated at about 8.6 for f

= 0.3 and Mw=9.0. The estimated Mj tends to the observed one. This suggests that the small Mj is due to the small Vr.
Note: *Yamamoto and Yabe, 2009; http://kynmt.in.coocan.jp/ ;(REFERENCE/23)
**http://www.jma.go.jp/jma/kishou/books/gizyutu/133/ALL.pdf

Keywords: Seismic efficiency, Moment magnitude, JMA magnitude, Slow slip event, Rupture velocity, Damagezone fault model of earthquake

Long-term seismic quiescence before the 2010 M_w8.8 Chile earthquake and the 2001 M_w8.4 Peru earthquake

*Kei Katsumata[1]

1.Institute of Seismology and Volcanology, Hokkaido University

An earthquake catalog created by International Seismological Center (ISC) was analyzed in the study area, 65°W to 80°W, 10°S to 60°S, between 1 January 1964 and 31 December 2009, including 1062 earthquakes shallower than 60 km with the body wave magnitude of 5.0 or larger. Clustered events such as earthquake swarms and aftershocks were removed from the ISC catalog by using a stochastic declustering method developed by Zhuang et al. (2002). A detailed analysis of the earthquake catalog using a gridding technique (ZMAP) shows that the seismic quiescence areas are found in and around the focal area of the 2010 M_w8.8 Chile and the 2001 M_w8.4 Peru earthquakes. The seismic quiescence area for the 2010 Chile earthquake is a circle centered at (36.7°S, 73.1°W) with a radius of 144 km. The seismicity rates in this area are 1.1 events/year between 1964.0 and 1990.4, 0.19 events/year between 1990.4 and 2004.3, and 0.83 events/year between 2004.3 and 2010.0. The seismic quiescence area for the 2001 Peru earthquake is a circle centered at (17.7°S, 72.1°W) with a radius of 113 km. The seismicity rates in this area are 0.76 events/year between 1964.0 and 1990.4 and 0.0 events/year between 1990.4 and 2000.5. In the case of the Chile earthquake the seismic quiescence ended six years before the main shock on 27 February 2010. On the other hand, in the case of the Peru earthquake the seismic quiescence ended at the almost same time as occurrence of the main shock on 23 June 2001.

Keywords: seismic quiescence, ZMAP, the 2011 Chile earthquake, the 2001 Peru earthquake

Influence of the 2011 Tohoku, Japan earthquake on the Korean peninsula

*Sun-Cheon Park[1], Jun-Whan Lee[1], Hyojin Yang[1], Eun Hee Park[1], Won-Jin Lee[1]

1.National Institute of Meteorological Research, Korea Meteorological Administration

The 2011 Tohoku, Japan earthquake (M9.0) not only produced catastrophic damage in Japan but influenced on the Korean peninsula in terms of the seismicity, tsunami and crustal deformation. Seismic waves were large enough to be saturated in broadband seismic stations equipped with STS-2 seismometer which were located in the eastern part of the peninsula. Also small tsunami waves were observed along the southern and eastern coast. We have analyzed the tsunami as well as the seismic activity and crustal movement to understand the influence of the Tohoku earthquake on the Korean peninsula which is located about 10~15 degrees far from the fault plane.
Tsunami generated by the Tohoku earthquake propagated to the Korean peninsula as well. Tsunami with the height of less than 30 cm was observed about 3~5 hours later at the water level stations in southern and eastern coast of the peninsula, as can be expected by numerical tsunami simulation. However, some water level changes occurred even a few minutes after the earthquake at the several water level stations in north-eastern part of South Korea. We calculated horizontal displacements as well as vertical ones in the surrounding seas of the peninsula using the slip distribution obtained by the seismic waveform inversion (Baag et al., submitted). Then the tsunami was calculated considering the bathymetry effect or the effect of the horizontal displacement and the seafloor slope, following Murotani et al. (2015). As the result, the unexpected tsunami observed a few minutes later seems to have a coincidence with the tsunami generated by the bathymetry effect.
The level of seismicity was changed by the Tohoku earthquake. Even though only three earthquakes with magnitude greater than 2 were reported by the Korea Meteorological Administration (KMA) within 5 days since the event, 53 events including micro earthquakes were identified using continuous waveforms only in the day of the earthquake (Park, 2012). Unusually large increase of seismic events was observed rather in 2013. Those events include three moderate earthquakes of M~5 and intensive swarm in the Yellow Sea region. Hong et al. (2015) interpreted that this phenomenon was induced by the fluid diffusion during the transient tension field and pore pressure increase during the ambient compressional-stress field recovery.
Crustal deformation was determined using the GNSS data densely distributed in the Korean peninsula. The displacements induced by the earthquake were about 1.5~4 cm. The crust moved toward the direction of the fault, which was to the east and it differs from the general movement of this region before the Tohoku earthquake. And the trend of eastward movement continued at least until 2012. The annual velocity of crustal deformation showed that the movement was recovered to the general direction since 2013.
These analyses indicate that the Tohoku earthquake has directly influenced on the Korean peninsula. And it may be necessary to consider the influence of another large earthquake that can be expected around the Japanese islands, like expected Nanakai earthquake.

Keywords: 2011 Tohoku, Japan earthquake, tsunami, crustal deformation, seismicity, Korean peninsula

Analysis of foreshock sequence of the 2014 M_w6.2 Northern Nagano earthquake: Implications for slow-slip transient and unusual source property

*Kazutoshi Imanishi[1], Takahiko Uchide[1]

1.Geological Survey of Japan, AIST

The M_w 6.2 Northern Nagano earthquake occurred on November 22, 2014, central Japan, which broke a northern part of the Itoigawa-Shizuoka Tectonic Line active fault system. The earthquake has a foreshock sequence from four days before the mainshock, which was captured by a dense permanent seismic observation. We first determined hypocenters of foreshocks, mainshock, and aftershocks by assuming two different one-dimensional velocity models to account for heterogeneous structure in the area. We then applied the double-difference (DD) method to improve the precision of event relative locations. The DD location reveals that the foreshocks were located at a depth of 3-4 km and distributed on a NNW dipping 1 km x 1 km plane with an angle of about 60 degree (plane A), which is distinct from the aftershock distribution. The geometry of the plane A is consistent with the foreshock focal mechanisms determined by P-wave polarities as well as body-wave amplitudes. We also found that the foreshock sequence is located at the eastern extension of two Neogene faults described in the geological sheet map at 1:50,000 (Geological Survey of Japan, 2002), where the strike of one of the faults agrees well with that of the plane A. These Neogene faults cut active folds as well as Otari-Nakayama fault, making the region become a local structural heterogeneity. We infer that the foreshock sequence appears associated with fault zone complexity, as suggested for other foreshock sequences (e.g., Chen and Shearer, 2013).
In order to investigate the foreshock sequence in more detail, we analyzed seismograms recorded at Hakuba Hi-net station, which is a 632-m deep borehole station located about 5 km west of the foreshock region. By a visual identification of running spectra at the Hakuba station and S-P time, we newly detected 384 foreshocks, which are nearly seven times more than those in the JMA catalogue. We determined their locations and magnitudes on the basis of waveform cross-correlations and amplitude ratios, respectively, between newly detected foreshocks and DD relocated events. Our new catalogue delineated another plane with a N-S striking vertical plane (plane B), which is consistent with one of nodal planes of the P-wave first-motion mechanism of the mainshock. The spatial and temporal distribution of our new catalogue indicates that the foreshock sequence started at the deeper part of the plane A, migrating to the shallower part, and then jumped to the plane B, migrating to the mainshock hypocenter. The migrating speed is less than a few km/day, implying a possible slow-slip transient. A hypothesis is that the foreshock sequence is driven by aseismic slip, which causes stress loading at the mainshock hypocenter and triggers the mainshock.
We further determined source parameters of the foreshocks to investigate their fault properties. We applied Multi-Window-Spectral-Ratio method (Imanishi and Ellsworth, 2006) to the foreshocks and aftershocks using the deep borehole data. The estimated corner frequencies of aftershocks decrease with magnitude and indicate constant stress drop. In contrast, the estimated corner frequencies of foreshocks are almost constant over nearly two orders of magnitude. The constant corner frequency suggests that fault dimension is the same regardless of magnitude or stress drop increases with magnitude under an assumption of scale-invariant rupture velocity. It is noted that the same observation was reported for the foreshock sequence of the 1999 M_w7.6 Izmit earthquake, Turkey (Bouchon et al., 2011), which may indicate that the constant corner frequency or the size-dependent stress drop is a common specific property of foreshocks.
Acknowledgements: Seismograph stations used in this study include permanent stations operated by NIED Hi-net, JMA, ERI, and DPRI.

Keywords: 2014 Northern Nagano earthquake, foreshock, source property, slow slip

Delayed triggering process of the M_{JMA}6.4 Eastern Shizuoka earthquake on March 15, 2011 by analyses of stress changes and detection of foreshocks

Rina Tamura[1], *Masatoshi Miyazawa[2]

1.Graduate School of Science, Kyoto University, 2.Disaster Prevention Research Institute, Kyoto University

We investigated the triggering process of the Mj6.4 Eastern Shizuoka earthquake on March 15, 2011, which occurred 4 days after the 2011 Mw9.0 Tohoku-Oki earthquake and about 4 minutes after the Mj6.2 Fukushima-Oki earthquake. We obtained a static Coulomb failure stress change on the fault of the Eastern Shizuoka earthquake by the Tohoku-Oki earthquake, which was about 21 kPa, and the largest dynamic stress change by the passing surface waves was about 200 kPa. The largest dynamic Coulomb failure stress change from the Fukushima-Oki earthquake and tidal stress change after the Tohoku-Oki and before the Eastern Shizuoka earthquake were about 0.3 kPa and 1.2 kPa, respectively, while those at the onset of the Eastern Shizuoka earthquake were negative values of about -0.01 kPa and -0.2 kPa. We also tried to detect earthquakes immediately preceding the Eastern Shizuoka earthquake using a matched filter technique and found one M1.0 event that located about 2 km NNE from the mainshock and occurred about 17 hours before it. However, this event may not be identified as a foreshock according to the background seismicity before 2011 in this region. We propose that delayed triggering (clock advance) might have occurred for the Eastern Shizuoka earthquake, where the frictional stress had rapidly built up due to these static, dynamic, and tidal stress changes when the eventual earthquake was ready to occur.

Keywords: Eastern Shizuoka earthquake, Delayed triggering, Coulomb failure stress change, Foreshock

Re-analysis of Seismic Quiescence and Slow Slip in Hamanako region

*Sumio Yoshikawa[1], Naoki Hayashimoto[1], Tamotsu Aketagawa[2]

1.Meteorological Research Institute, 2.Okinawa Regional Headquarters

We have shown a remarkable spatial correlation between the seismic quiescence in the Philippine Sea plate and the Long-term Slow Slip Event (LSSE) in the plate boundary beneath Hamanako region, though did not have shown a clear time correlation between them (SSJ, 2015). Against this, according to JMA (since September 2014), the seismicity in the crust of the central western Shizuoka becomes low simultaneously with two times of LSSE in the plate boundary beneath Hamanako region, which suggests a clear time correlation between the seismic quiescence and LSSE. On the other hand, Kobayashi and Yoshida (2004) and Yamamoto et al. (2005) have pointed out occurrence of LSSE in the period from 1988 to 1990. If LSSE are repeating similarly in this region, it is important to clarify how LSSE can be caused at the same time when the quiescence in the crust of the central western Shizuoka appears, and to make clear the reason why we cannot observe a clear time correlation between the seismicity and LSSE beneath Hamanako region.

We used the eMAP technique (Aketagawa and Ito, 2008; Hayashimoto and Aketagawa, 2010) for space time analyses of seismic quiescence and activation. The attached figure shows source distribution maps of seismic quiescence and activation detected by the eMAP for the earthquakes with the magnitude equal to and larger than 1.1 in the central western Shizuoka and around Hamanako. The epicenter map (a) shows concentration of quiescence areas near the Suruga bay and around Hamanako. The vertical cross section (b) shows a clear quiescence beneath Hamanako region and activation zones beneath the central western Shizuoka both in the crust and the plate. The activation seems to reflect the seismic activity in a part of the locked zone of the plate boundary inferred by Matsumura (1997). The space time plot (c) shows activation in the SE part continues from 2006 to 2012, whereas it becomes relatively low in the periods from 2001 to 2005 and from 2013 to present, at the same time when LSSE is observed, which supports correspondence of the low seismicity in central western Shizuoka with LSSE as it was pointed out by JMA. Against this, quiescence around Hamanako region is not clearly correspondent with LSSE, though the area of quiescence seems inferior for the rest of LSSE from 2006 to 2012.

We then searched seismic quiescence that previously occurred in the same area from January of 1983 for the earthquakes with the magnitudes equal to and larger than 2.3. As a result of this we confirmed an example also in the period from 1988 to 1990 in a small region of the same area. This result may indicate the possibility that the quiescence in the locked zone occurred with LSSE in the plate boundary beneath Hamanako region as many as three times.

It is possible to explain the mechanism for the correspondence of the quiescence with LSSE if the stress reduction in the locked zone occurs at the same time when LSSE makes stress release in the plate boundary, though it is still complicated to tell the reason why no clear time correlation is found between quiescence and LSSE in the plate beneath Hamanako region. It may be necessary to make more analysis for the seismic activity based on stress distribution caused by heterogeneity within the crust and the plate.

Keywords: Seismic quiescence, Seismic activation, Slow slip event

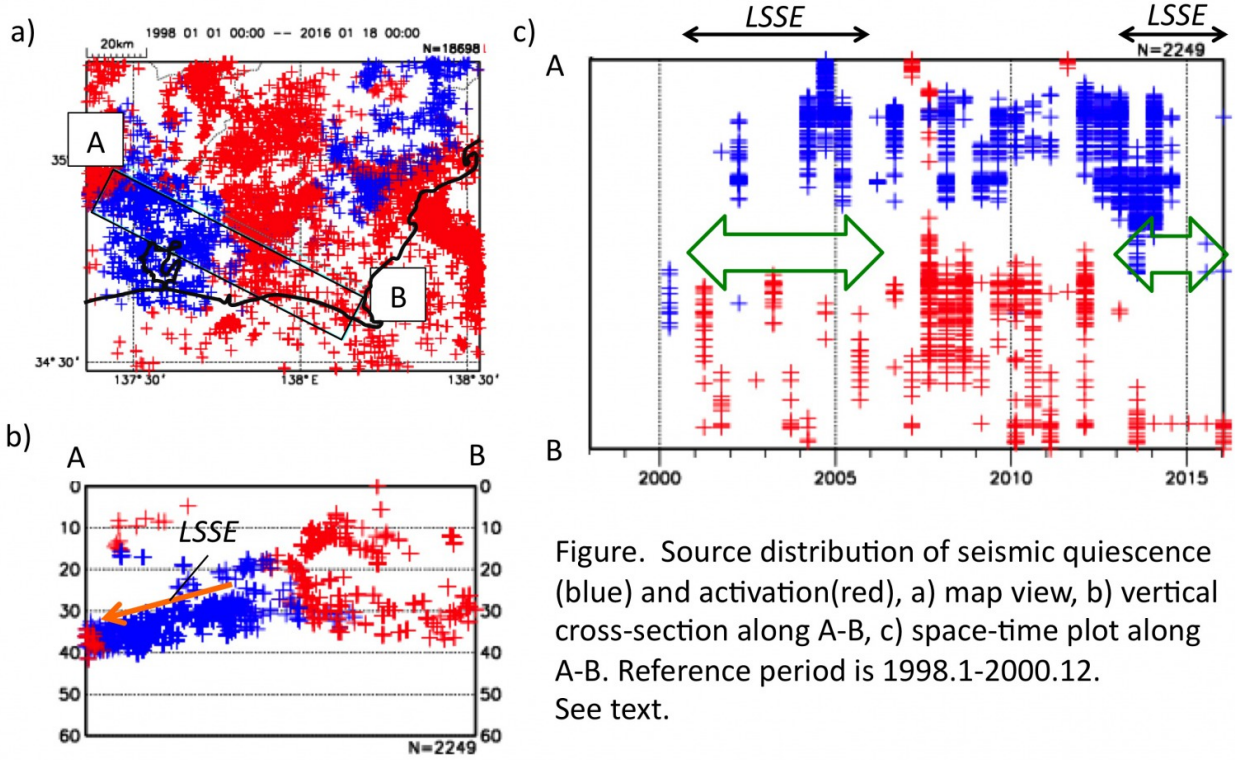

Figure. Source distribution of seismic quiescence (blue) and activation(red), a) map view, b) vertical cross-section along A-B, c) space-time plot along A-B. Reference period is 1998.1-2000.12.
See text.

Temporal change of focal mechanism pattern in the Tohoku-oki region

*Hiroaki Matsukawa[1], Yuji Yagi[1], Bogdan Enescu[1]

1.Geoscience, University of Tsukuba

It is well known that after the occurrence of a megathrust earthquake, a pattern of focal mechanisms of subsequent events changes since stress field near the hypocenter is significantly changed. For example, in the case of the 2011 Tohoku-oki earthquake, the number of normal-fault earthquakes increased after the mainshock (e.g., Asano et al., 2011) . Temporal change of the focal mechanism reflects the stress accumulation / release process in-between the megathrust earthquakes and the stress state recovery after the mainshock to pre-mainshock condition. However, there are still few studies discussing the temporal change of focal mechanism at high time resolution. In order to track the temporal change of stress field near the source area of the 2011 Tohoku-oki, we focused on the temporal change of the focal mechanisms in the 2011 Tohoku-oki region.
First, we classified the faulting type of earthquakes in the F-net catalog (National Research Institute for Earth Science and Disaster Prevention) as normal fault, thrust fault and strike-slip fault by following the method of Frohlich (1992) . The time window for sampling was fixed to 10 days for after the mainshock and 50 days for before the mainshock. In order to stabilize the temporal change, we defined a sampling sequence so we can include a number of earthquakes more than 500 for after the mainshock and mone than 100 for before the mainshock.
The results show that the ratio between the number of normal fault earthquakes to the total earthquakes increases step-wise after the mainshock and gradually decays with time. The gradual decay of the ratio has significant fluctuations and did not reach yet the level before the mainshock. The phenomenon of gradual recovery may reflect the flow of asthenosphere and after slip in deeper area of the hypocenter. It may also reflect changes of stress in the subducting and overriding plate. Moreover, focusing on before the mainshock, we observed the rapid decrease of the ratio. The same phenomenon was not observed from 1997 (start observation by F-net) to before the mainshock. This rapid decrease may relate to the preparation process of the 2011 Tohoku-oki occurrence.

Keywords: focal mechanism pattern, temporal change of focal mechanisms, 2011 Tohoku-oki earthquake

Sequence of moderate-to-large deep focus earthquakes around Off Ogasawara Islands on 23th June 2015

*Shunsuke Takemura[1], Tatsuhiko Saito[1], Katsuhiko Shiomi[1]

1.National Research Institute for Earth Science and Disaster Prevention

Large deep-focus earthquake with Mw 6.5 occurred around Off Ogasawara (Bonin) Islands, at 21:18 (JST) on 23th June 2015. Observed seismograms of Hi-net, which contain several *P* and *S* waves arrivals during 10 minutes from 21:18 (JST), indicate that relatively large earthquakes sequentially occurred around Japan. In this study, using velocity seismograms of F-net and Hi-net, we investigate seismic wave propagation during sequential earthquakes and estimate the magnitude of each event.

To clarify how seismic waves propagate across Japan during earthquake sequence, we made snapshots of seismic energy propagation by using mean-square (MS) envelopes of Hi-net waveforms. MS envelopes were calculated by sum of three-component filtered seismograms with passed frequency of 1-32 Hz. Then, we took spatial interpolation of amplitudes of MS envelopes at each time step to make smooth spatial distribution of seismic energy at each time step. Snapshots of seismic energy propagation visually show that one earthquake occurred around Sea of Japan and then three earthquakes occurred around Off Ogasawara Islands. Second Off Ogasawara event was not listed in the JMA PDE catalogue. Since the propagation patterns of seismic energy of three earthquakes around Off Ogasawara are very similar, we consider that these earthquakes have similar hypocenter locations. Then, to evaluate magnitude of detected events, we measured maximum S wave amplitudes of each earthquake from MS envelopes at F-net station and calculated amplitude ratio with maximum S wave amplitude of first earthquake, which has a seismic moment of 5.47×10^{18} Nm (Mw6.5) referred from CMT solution of F-net. Amplitudes ratio and estimated seismic moment are 0.462 ± 0.023 and $2.52 \pm 0.13 \times 10^{18}$ Nm (Mw6.2±0.1) for second earthquake, respectively, and 0.106 ± 0.004 and $5.80 \pm 0.22 \times 10^{17}$ Nm (Mw5.8±0.1) for third earthquake, respectively.

Acknowledgement

We use the Preliminary Determined Earthquake catalogue provided by the Japan Meteorological Agency.

Keywords: deep focus earthquake, seismic wave propagation, seismogram envelope, Izu-Bonin arc

Operation of the SWIFT CMT analysis system in Colombia and characteristic of seismicity in the complex subduction zones

*Masahiro Yoshimoto[1], Hiroyuki Kumagai[1], José Faustino Blanco[2], Yuta Maeda[1], Viviana Dionicio[2]

1.Nagoya University, 2.Servicio Geológico Colombiano

Colombia is located in the triple junction of the Nazca, Caribbean, and South American plate, and the complex plate subductions cause various seismicity pattern. The great earthquakes such as the 1906 Ecuador-Colombia earthquake (Mw8.8) and the 1979 Tumaco (south west of Colombia) earthquake (Mw8.2) occurred at the boundary between the subducting Nazca plate and the South American plate. There are no historical records of large earthquakes in the northern part of the boundary, and a potential for a future large earthquake is unresolved issue. An intermediate earthquake concentration known as the Bucaramanga nest is observed in the inland region. The 1967 M6.3 earthquake of the nest also caused much damage in Bucaramanga. However, most of nest earthquakes are not included in the global CMT catalog because of their small magnitude. Despite highly concentrated seismicity in the nest, the CMTs reported in the global CMT catalog also indicate various focal mechanism. This may causes difficulty in understanding the nature of the nest. To understand the nature of the nest activity and the complex plate interactions, it is very important to determine the focal mechanisms including small events.
The JST/JICA SATREPS project of "Research and development of disaster mitigation techniques of earthquake, tsunami, and volcano in Colombia" was started in 2015. We installed the SWIFT system (Nakano et al., 2008) in the Colombia Geological Survey and determined CMT solutions and source time functions of the Colombian regional earthquakes. We now carry out the following studies: 1) detection of very low frequency (VLF) earthquakes and tremors in Colombia, 2) determination of CMT solutions including small events which are not listed in the global CMT catalog. Although we have not been able to detect any VLF events until now, we obtained CMT solutions including small events by the SWIFT. The smallest magnitudes are Mw4.3 for shallow events and Mw4.6 for intermediate depth events. The global CMT catalog shows that the focal mechanisms in the Bucaramanga nest are highly variable, but our many CMT solutions show the mostly strike-slip faulting with some dip-slip components and SW-NE directions of P axis. Other events show focal mechanisms opposite to these mechanisms. Prieto et al. (2012) found repeating and "anti-repeating" earthquakes in the nest and suggested that the nest is not a volumetric but a planar seismic activity. Our results also support their idea, but we need more information of further past events. Toward understanding the nature of the nest and the complex subduction processes, we will also analyze the focal mechanisms of smaller events using P wave polarities.

Keywords: SWIFT, Colombia, seismicity

A dense seismic array observation across the central focal area of the 2015 Gorkha earthquake(Mw 7.8), Nepal

*Eiji Kurashimo[1], Hiroshi Sato[1], Shin'ichi Sakai[1], Naoshi Hirata[1], Hiroshi YAGI[2], Ananta Prasad Gajurel[3], Danda Pani Adhikari[3], Krishna Subedi[4], Bishal Nath Upreti[4]

1.Earthquake Research Institute, the University of Tokyo, 2.Yamagata University, 3.Tribhuvan University, 4.Nepal Academy of Science and Technology

On April 25, 2015, the Gorkha earthquake (Mw 7.8) struck central Nepal and resulted in nearly 9000 fatalities. This earthquake occurred in the India-Eurasia Plate Collision Zone. The focal mechanism showed a reverse fault with a compression axis in a NNE-SSW direction (USGS, 2015). The Himalayan seismogenic zone is located in a typical continental collision zone. Several geological cross sections through the central Himalaya have been proposed (e.g., Cattin and Avouac, 2000, JGR). However, little is known about the detailed geophysical structure of the India-Eurasia plate collision zone. Moreover, the 2015 Gorkha earthquake failed to rupture to the surface and hence a large earthquake appears to be inevitable (Bilham, 2015). Revealing the crustal structure of the India-Eurasia plate collision zone is important to constrain the process of earthquake occurrence and the crustal evolution process associated with the collision of the continents. To investigate aftershock distribution and crustal structure, we conducted a dense seismic array observation across the central focal area of the 2015 Gorkha earthquake. Thirty-five portable seismographs were deployed along a 90-km-long line between Shabru Besi and Hetauda. Each seismograph consisted of a 4.5 Hz 3-component seismometer and a digital data recorder (GSX-3). Waveforms were continuously recorded at a sampling rate of 250 Hz for one month. Recordings were started on August 15, 2015 and November 28, 2015. In this presentation, we present precise aftershock distribution and seismic velocity structure across the central focal area of the 2015 Gorkha earthquake.

Keywords: The 2015 Gorkha earthquake, India-Eurasia Plate Collision Zone, dense seismic array observation, aftershock distribution

Monitoring of Background Seismicity and Induced Earthquakes Associated with Enhanced Geothermal Systems in Ilan, Taiwan

*ShueiHuei YOU[1], Laetitia Mozziconacci[2], Yuancheng Gung[1], MengChieh Tsai[1], ChingYu Lu[1]

1.National Taiwan University, 2.National Taiwan Ocean University

Hydro-fracturing stimulation is one of the key steps in the development of EGS. It aims to create a subsurface system full of cracks and fractures, thus providing an efficient water channel network to enhance the thermal energy extraction. Since small earthquakes are triggered by the occurrence of rock fracture, the distribution of hydro-fractures can be delineated by locations of these induced earthquakes. In this project, we have deployed 6 bore-hole seismometers to accurately capture the weak signals from these micro events. The influence on local seismicity from water-pumping is another important issue in this project. Preliminary analysis of data from our own borehole network indicates that many recorded local micro events are not reported in the CWB catalogue, thus, we need to rely on the borehole data to better evaluate the local background seismicity. We have also analyzed data during the stimulation experiments conducted in 11/09, 11/13 and 11/14, 2014. After various examinations, we noticed two major signals during the stimulations, the tremors, which are likely induced by water-pumping, and the free-oscillations of the water-filled cracks, which are obviously enhanced during the pumping period. However, probably because the energy from the induced rock failure is too weak, these signals were only recorded by the nearest borehole station, and there is no clear arrival time in the tremor signals. During the period from October 2014 to November 2015, 1313 local earthquakes were recorded by the bore-hole seismic network. We first determined the seismic velocity of the shallowest layer (depth < 500 m) with applying ambient noise technique on seismic records of local earthquakes, and inverted a minimum velocity model and preliminary locations of earthquakes by using the package VELEST developed by Kissling. We then relocated local earthquakes using “HYPODD” technique, and calculated local magnitude (ML) of these events. Most of these events are located at depth less than 5 km with rather small magnitudes (ML<1.0). Our results have well demonstrated that we are able to improve local micro-earthquake monitoring by using the bore-hole seismic network. During the stimulation experiments, no apparent variations of seismicity were noticed. Interestingly, the seismicity right beneath the injection well (2 –5 km) was clearly increased 3 days after the pumping, and such phenomena lasted for about 10 days. Besides the seismic swarm related to the stimulation experiments, we also identified several seismic swarms at shallow depth which imply relatively active geological structures in the study area.

Keywords: borehole seismometer, induced earthquakes, focal mechanism of micro-earthquake

Focal Mechanisms and Seismicity in the Region of Induced Earthquakes of Song Tranh Dam, Vietnam

*Cuong Quoc Nguyen[1]

1.DPRI Kyoto University

Vietnam is located in South East Asia and bounded by the Pacific and Mediterranean-Himalaya seismic belts on its eastern, western and southern sides, respectively. The dynamic tectonic processes in this region cause the territory of Vietnam and adjacent areas to have intensive differential movement, making the regional tectonic structure very complicated. The tectonics have led this territory to have moderate seismic activity and complicated geological structures, such as the Lai Chau-Dien Bien fault zone, Red River fault zone, and others. Southern Vietnam was considered to be a region with low seismicity, compared to the North. However, the sequence of earthquakes that occurred at Song Tranh Dam during the last several years surprised many scientists because the southern region of Vietnam was not expected to have major tectonic activity. This region where many induced earthquakes are now occurring is associated with the filling of a new reservoir. There have been four M4 earthquakes (maximum earthquake was 4.7 in November, 2012), so it is one of the most active induced earthquakes examples in the world. It is important to determine the strong motion attenuation relations for this area since damaging earthquakes may be expected in the near future. We collect and process data from 5 seismic stations around Song Tranh dam, include more than 300 events larger than 1.5 and more than 2000 seismic waveforms to determine arrival times and locate the earthquakes in the Song Tranh dam region. In this study we use time domain analyses to determine focal mechanisms. We use software of Dreger and Ford (2011) modified for the Song Tranh Dam region. Induced earthquakes processed by this software include events withmagnitudes larger than 3.5 and recorded on 4 or more stations.
We also compare our results with mechanisms for tectonic earthquakes in the region (Hung Nhuong Tavi and Tra Bong faults). The results show a difference in focal mechanism between tectonic earthquakes and induced earthquakes which may be related to the increased fluid pressure from filling of the reservoir. To confirm this result, we will need to process the many smaller events with magnitude less than 3.0, which have occurred around Song Tranh Dam.
We used a genetic algorithm method to estimate the local velocity structure. We applied this method to determine a layered model for the Song Tranh dam region. Our results obtained a new 1D model of 7-8 layers. The shallow P wave velocity of 4.6 km/s is slower than 5.9 km/s for previous studies in northern VietNam. For a deeper layers from 6 to 12 km, P wave velocity becomes larger, 5.4 km/s –5.9 km/s. The Vp/Vs shows relatively higher values of 1.75-1.77 for the depth around 12 km. When layer thickness changes from 21 km to 28 km, the P wave velocity increases and changes from 6.5 km/s to 7.3 km/s, however, Vp/Vs ratio decreases from 1.77 to 1.67. Finally, the depth of the Moho surface changes from 28 to 35 km and the P wave velocity changes from 7.8 to 8.2 km/s, with Vp/Vs value of about 1.78. Earthquakes still occur at Song Tranh dam (a recent M3.3 occurred on August,26 th 2015), and more than a thousand earthquakes with magnitude less than 1.5 have not yet been processed. We continue to update the seismic analyses with information from smaller earthquakes to improve our results.

Keywords: Song Tranh Dam, Focal Mechanism, Velocity structure, induced earthquake

Detectability of temporal variation of b-value prior to two earthquakes (Mj6.3 in 2013, Mj5.1 in 2014) in Northern Tochigi Prefecture

*Naoaki Yoneda[1], Hironori Kawakata[1], Shiro Hirano[1]

1.Department of physical Science, College of Science and Engineering Ritsumeikan University

It has been reported that the b-value decreases prior to large earthquakes in nature (e.g., Imoto, 1991) and failure of a rok sample in laboratories (e.g., Scholz, 1968) . To discuss a temporal variation of the b-value, a sufficient number of earthquakes is required. In general, calculation of b-value prior to large earthquakes requires long-term data because seismic activity is not always high at that term. In other words, the temporal resolution of b-value variation before a large earthquake is usually low. Therefore, sufficiently high seismic activity before the large earthquake is required to evaluate the b-value variation precisely.
For example, two major earthquakes occurred in northern Tochigi Prefecture: Mj6.3 in 2013 and Mj5.1 in 2014. The two events followed the increase of seismic events. One possible cause of this increase is the Mw9.0 Tohoku earthquake in 2011 (e.g., Aketagawa, 2011).
In this study, we try to detect the temporal variation of the b-value in northern Tochigi Prefecture where a large number of earthquakes could be observed in a short period prior to the two major events. First, to increase the temporal resolution, we calculate the b-value for a circular region with 20km radius from the epicenter of the Mj6.3 event; the result is shown in Figure A. While the b-value was greater than 1.0 and stable before March 2011, it dramatically decreased to ~0.6 after the occurrence of the Tohoku earthquake in 2011 and recovered to around 1.0 almost within one year. After that, it decreased to ~0.7 again following the Mj6.3 event in 2013 and recovered to ~1.0 within a small period. Although it decreased to ~0.75 again following the Mj5.1 event in 2014, it did not recover but continued, at least, one year. Regarding these different variations in each sequence, we considered the seismic activity in northern Tochigi precisely. We consider regions 1, 2, and 3. The region 1 is located south of the source region of the Mj6.3 event and includes an active fault. The regions 2 and 3 include the source areas of the Mj6.3 and Mj5.1 events, respectively. The temporal variation of b-value for each region is shown in Figure B, C, and D. In region 1, constant seismic activity has continued for the whole term and the b-value was stable and greater than 1.0. The b-values are also stable but ~1.0 in region 2 and ~0.75 in region 3. On the basis of these results, we found that the temporal variation of the b-value of the entire region is affected by the temporarily activated one of the three regions. However, in regions 2 and 3, the numbers of events to calculate the b-value precisely are insufficient despite their activation. So we found that we cannot detect temporal variation of the b-value prior to the major events. This finding tells us that we need to consider the target region carefully when we research the temporal variation of the b-value.
Acknowledgments
In this study, we used the JMA unified hypocenter catalogue.

Keywords: b-value, Northern Tochigi Prefecture, seismic activity

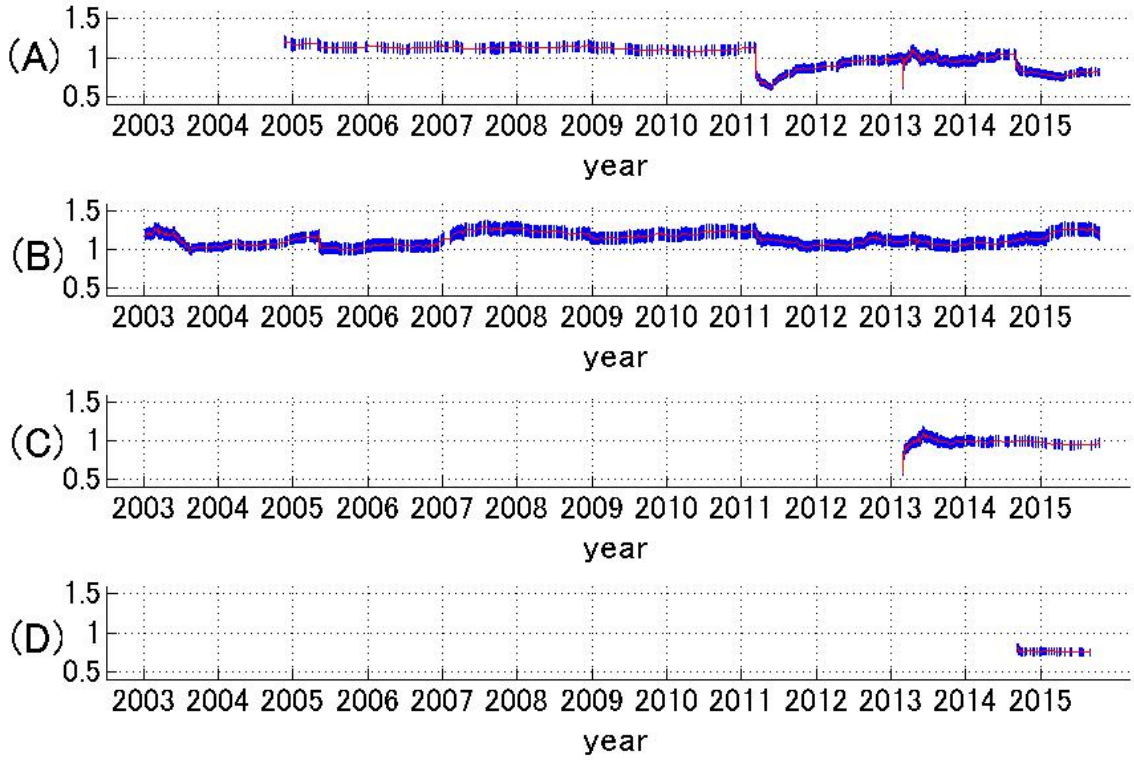

Spatiotemporal variation of earthquake-tide correlations after the 2011 Tohoku earthquake

*Sachiko Tanaka[1], Youichi Asano[1]

1.National Research Institute for Earth Science and Disaster Prevention

We examined correlations between tides and earthquakes off the Pacific coast of eastern Japan for about five years after the 2011 Tohoku earthquake (Mw 9.1). A previous study by Tanaka (2015) using the earthquakes with Mw 5.0 or larger in the Global Centroid Moment Tensor (CMT) catalog after the Tohoku earthquake showed significant correlations on the northwest side of the large-slip area of the Tohoku mainshock, where large postseismic afterslip has been identified by geodetic measurements (Ozawa et al., 2012; Sun et al., 2014). In the present study, we extend this work to a larger catalog including smaller earthquakes, to more thoroughly explore the earthquake-tide correlations. In about ten years prior to the Tohoku earthquake, high correlations were observed in the northern part of the Tohoku source area where the mainshock rupture initiated (Tanaka, 2012); however, those correlations could not be seen with smaller earthquakes (Tanaka and Asano, 2012).

The data we used are the CMT solutions of 1068 interplate earthquakes with Mw 4.0 or larger from the Tohoku earthquake to December 2015, which were determined by the waveform inversion of seismograms from the NIED Hi-net and F-net stations (Asano et al., 2011). Based on tidal phase angles at the earthquake origin times derived from theoretically-calculated tidal Coulomb failure stresses with a friction coefficient of 0.2 (Tanaka et al., 2012), we evaluated the Shuster's p-value (Schuster, 1897), which represents the significance level to reject the null hypothesis that the earthquakes occur randomly irrespective of the tidal phase angle.

We examined the spatial distribution of p-value using the 200 km x 200 km moving windows for the period after the Tohoku earthquake. The results indicate significant correlations on the south side of the Tohoku large main-slip area. The smallest p-value of 0.52% was observed in the window located off Ibaraki prefecture. The temporal variation of p-value in this region shows the p-value was larger than 10% just after the Tohoku earthquake and gradually decreased with time. The p-value in the latest 700 days is 0.09%. When using only larger earthquakes, we found no significant correlation in this region; we can see p-values smaller than 5% with the earthquake magnitude cutoff smaller than 4.8.

On the other hand, with increasing the earthquake magnitude cutoff, we observed high correlations on the northwest side of the Tohoku large slip area. The highest correlation was seen when the magnitude cutoff was set to be 4.8, and the smallest p-value of 0.63% was obtained in the window located near the coast off Iwate prefecture. The area of high correlation is well correlated with the large afterslip area (Ozawa et al., 2012; Sun et al., 2014), as documented in the previous work (Tanaka, 2015). The temporal variation of p-value shows that the p-value was smallest (0.12%) just after the Tohoku earthquake and gradually increased with time. No significant correlation was found after 2014 in this region.

Keywords: the 2011 Tohoku earthquake, earth tides, earthquake triggering

Retrospectively forecasted seismicity in eastern Japan using spatio-temporal kernel smoothing

*Yuichi Ohkubo[1], Shinji Toda[1]

1.Graduate School of Science, Tohoku University

The best and pervasive statistical model to describe seismicity is the ETAS (Epidemic Type Aftershock Sequence) model (Ogata, 1988) which is based on modified Omori law and explain secondary aftershocks together with background seismicity. The ETAS model better explains mainshock-aftershock sequence but does not always fit earthquake swarm. Helmstetter and Werner (2014) instead proposed a simple, nonparametric model using a spatio-temporal kernel smoothing, without using the modified Omori law.

We applied the smoothing kernel model not only to the mainshock-aftershock type sequences, such as the Tohoku-oki earthquake (2011.3.11 M9.0) and the Iwate-Miyagi Inland earthquake (2008.6.14 M7.2) but also to a significant earthquake swarm in the Izu Peninsula that occured in 2000 to compare with the ETAS model. As a result, our kernel model for the mainshock-aftershock type earthquake performed almost same accuracy as the ETAS model did, except the significant underestimate immediatery after mainshock. Furthermore, the case of Tohoku-oki earthquake that a large foreshock (2011.3.9 M7.3) was observed, the number of predicted earthquakes became several hundred times higher than the background rate during the time period between the foreshock and M9 mainshock. Although the probability gain was about several hundred times higher than the one in a few days after the Iwate-Miyagi Inland earthquake, probability gain was low in a few days after the Tohoku-oki earthquake compared to that for the Iwate-Miyagi Inland earthquake. Because we applied the two-dimentional model only using earthquakes shallower than 30 km, the prediction accuracy of the interplate earthquakes is lower than that of the inland earthquakes. In the case of the earthquake swarm occurred in the Izu Peninsula, our kernel model was able to better estimate the seimicity than the ones by the ETAS model.

Keywords: smoothing, aftershock, earthquake swarm

Quantification of the cross-correlation criteria for small foreshock detection

*Yutaka Toyomoto[1], Hironori Kawakata[2], Shiro Hirano[2], Issei Doi[3]

1.Graduate School of Physical Science and Engineering, Ritsumeikan University, 2.Department of Physical Science, College of Science and Engineering, Ritsumeikan University, 3.Disaster Prevention Research Institute

Recently, small foreshocks have been frequently detected using a cross-correlation technique (e.g., Bouchon et al., 2011, Science). For inland earthquakes, foreshocks whose hypocenters were estimated to be adjacent to the mainshock hypocenter were detected from several tens of minutes before the main shock occurrence (Doi and Kawakata, 2012, GRL; 2013, EPS). Toyomoto et al. (2015, SSJ) tried to detect foreshocks of an M 5.4 earthquake in central Nagano prefecture on June 30, 2011, in a similar manner to Doi and Kawakata (2013). Using the continuous waveforms of the vertical component at N.MWDH (Hi-net) station (the epicentral distance of the mainshock is 4.5 km), they newly detected 14 foreshocks with a cross-correlation criterion of 0.6, in addition to 27 foreshocks listed in the JMA (Japan Meteorological Agency) unified hypocenter catalogs. To efficiently detect small foreshocks for other inland earthquakes, it is necessary to design how to set the cross-correlation detection criterion for foreshock detection.
In this study, we carried out foreshocks detection of the same earthquake in the same method as Toyomoto et al. (2015, SSJ) using the waveform record of N.MNYH (Hi-net) station (epicentral distance of main shock is 5.3km). In this case, the maximum correlation coefficients during one minute tended to be higher than those for records at N.MWDH station, and the result of detection strongly depends on a threshold employed in a cross-correlation method. This indicates that we should not use a universal threshold independent of data. One of alternative way is to use the standard deviation of cross-correlation coefficients. Then, we made a histogram of the cross-correlation coefficients of 1-day data. The histogram of N.MWDH data is Gaussian and the cross-correlation coefficients obey a normal distribution with the average of zero. Although the histogram of N.MNYH data is not Gaussian, so the cross-correlation coefficients have a large-deviation. In such a case, a criterion depending on the standard deviation is inadequate.
Acknowledgments:
We used continuous waveform records of NIED high-sensitivity seismograph network in Japan (Hi-net) and the JMA unified hypocenter catalogs.

Keywords: foreshock, cross-correlation, detection criteria

Improvement of determination of hypocenters by pop-up type ocean bottom seismographs near Ogasawara Islands

*Kenji Nakata[1], Akio Kobayashi[1], Kazuhiro Kimura[1], Hisatoshi Baba[2], Yutaka Nagaoka[3], Hiroaki Tsushima[1], Akio Katsumata[1], Kenji Maeda[1]

1.Seismology and Tsunami Research Department, Meteorological Research Institute, Japan Meteorological Agency, 2.Department of Marine and Earth Science, Tokai University, 3.Volcanology Research Department, Meteorological Research Institute, Japan Meteorological Agency

There are only three permanent seismic stations in Ogasawara Islands, two Chichi-jima and one Haha-jima stations. Hypocenters, therefore, can be poorly determined in regard to locations of the east-west direction.
Meteorological Research Institute (MRI) deployed pop-up type Ocean Bottom Seismographs (OBSs) to investigate the more accurate locations of hypocenters than JMA catalogue in this area. The observation network covers the area of the range 26-29°N and 140-143°E. Observation period was from 15 Jul. to 10 Oct., 2015. We analyzed the eight continuous data at OBS stations and determined the hypocenters. We compared hypocenters determined by the OBS data with those of JMA catalogue. We extracted 31 events as the same events whose difference between the origin time by the OBS and the JMA are within three seconds. The hypocenters by the OBS tend to be shifted by 30′to 1°westward from those of the JMA. Its tendency is same as the result between hypocenters by the USGS and the JMA. It suggests that the locations of hypocenters can be improved by applying the results to the data of only permanent stations.

Keywords: Determination of hypocenters, Ocean Bottom Seismographs (OBSs), Ogasawara Islands

Determination of focal mechanism solution using simulated annealing

*Masanao Komatsu[1], Hiroshi Takenaka[1]

1.Graduate School of Natural Science and Technology, Okayama University

Many seismologists have determined focal mechanism solutions using grid search (e.g. Nakamura and Mochizuki, 1988, QJS) or genetic algorithms (e.g. Kobayashi and Nakanishi, 1994, GRL). However, simulated annealing (SA) that is known as one of the efficient methods for global optimization has never been used to determination of this solution, although it allows for getting an optimal solution by jumping out of local minimum. In this study, we apply the SA to determination of focal mechanism solution. When we express the null, pressure and tension axes using a set of Euler angles (e.g. Nakamura and Mochizuki, 1988), the optimal set of Euler angles is determined by minimizing difference between synthetic and observed polarity of P-wave first motion. To investigate the feasibility of the application, we determine focal mechanism solution of the 14 March 2014 Iyo-Nada intermediate-depth earthquake (M_{JMA} 6.2). The computation of SA method is then about the 1278 time faster than the grid search method. Strike, dip and rake angles calculated by the optimal set of Euler angles is nearly identical to focal mechanism reported by the Japan Meteorological Agency (JMA).
Acknowledgements: We used JMA Unified Hypocenter Catalogs. We also used a computer program disclosed by CSIRO for simulated annealing.

Keywords: focal mechanism solution, simulated annealing, grid search

The 2011 M6.4 Shizuoka earthquake sequence: triggering process investigation

*Anca Opris[1], Bogdan Enescu[2], Yuji Yagi[2], Sachiko Tanaka[3], Katsuhiko Shiomi[3]

1.Earth Evolution Sciences, Graduate School of Life and Environmental Sciences, University of Tsukuba, 2.Faculty of Life and Environmental Sciences, University of Tsukuba, 3.National Research Institute for Earth Science and Disaster Prevention

Many inland areas in Japan were seismically activated following the 2011 M9.0 Tohoku-oki earthquake. The activation mechanism includes triggering by dynamic, static or fluid-induced stress changes (e.g., Toda et al., 2011; Miyazawa et al., 2011; Shimojo et al., 2014). In this study we aim to understand the triggering processes associated with the 2011 M6.4 Shizuoka earthquake sequence; the mainshock of the sequence occurred on March 15, close to Mt. Fuji.
To improve the detection of smaller earthquakes, we have applied the Matched Filter Technique (MFT; Peng and Zhao, 2009) for the time interval from the Tohoku-oki earthquake until seven hours after the Shizuoka earthquake. We used Hi-net (NIED) continuous waveform data and seismograms of 1126 template events with M >= 1.0, which occurred in the study area between 2001 and 2014. The total number of Hi-net stations used was 25, selected within a 40 km radius from the main shock.
No foreshock activity was detected prior to the March 15 Shizuoka earthquake, which contrasts with other similar inland seismicity activations following the Tohoku-oki earthquake (e.g., Kato et al., 2013; Shimojo et al., 2014). Since the co-seismic static stress change due to the Tohoku-oki earthquake on the Shizuoka fault plane was significant (~0.5 bar), we argue that this is likely the most significant triggering mechanism and the delay of this sequence could be explained by the rate-and-state friction law (Dieterich, 1994).
The aftershock detection for the first 7 hours following the M6.4 event was significantly improved. When looking at the space-time distribution of the MFT detections, we observe that the earliest aftershocks (first minutes after the Shizuoka earthquake) occur to the north, close to Mt. Fuji, likely due to a stress increase from the Shizuoka mainshock. Indeed, by comparing the locations of these events with the slip model of Shizuoka earthquake derived from strong-motion data (JMA, 2011), we observe that they occur at the tip of the mainshock rupture.
The largest earlier aftershocks (M >= 4.0) occur as well in the north region. Aftershock distribution and focal mechanism data suggest that the northernmost earthquakes may have occurred on a different fault segment.
We also detect a rather gradual expansion of the aftershock distribution to shallower depths; the delay of activation in the shallow part remains to be further explored.

Keywords: seismicity, 2011 Shizuoka earthquake, triggering

Re-evaluation of Hypocenter of the Sakurajima Earthquake on January 12,1914

*Makoto Ogata[1], Satoshi Iwata[2], Kazuhiko Goto[3]

1.Kagoshima Local Meteorological offices,JMA, 2.Fukuoka Regional Headquarters,JMA, 3.NOEV, Kagoshima Univ.

The hypocenter of the Sakurajima Earthquake on January 12,1914 is Kagoshima-Bay in general. The 100th anniversary passes from 1914 Eruption of Sakurajima, we determine hypocenter of this earthquake by using selected S-P time data not only reported ones but also re-measured from smoked-paper seismograms. As a result, the hypocenter is revealed near by Kagoshima-city. The direction of first motion of smoked-paper seismogram recorded at of the Kagoshima meteorological observatory shows the hypocenter being located SE from the Kagoshima meteorological observatory.

Keywords: The Sakurajima Earthquake on January 12,1914, smoked-paper seismogram record, first motion analysis, S-P time (Duration of Preliminary Tremor), hypocenter determination

Nucleation Process of the 2011 Mw6.2 Northern Nagano Earthquake

*Kengo Shimojo[1], Bogdan Enescu[2], Yuji Yagi[2], Tetsuya Takeda[3]

1.Graduate School of Life and Environmental Sciences Doctoral Program in Earth Evolution Sciences University of Tsukuba, 2.Faculty of Life and Environmental Sciences University of Tsukuba, 3.National Research Institute for Earth Science and Disaster Prevention (NIED)

Introduction. Previous research.

An Mw6.2 inland earthquake occurred in northern Nagano region, central Japan, about 13 hours after the Mw9.0 Tohoku-oki megathrust earthquake. The regional seismic activity recorded in the Japan Meteorological Agency (JMA) catalog in the first hours following the megathrust event was highly incomplete, thus not allowing a detailed analysis of triggering mechanisms. By applying a Matched Filter Technique (MFT) to the continuous Hi-net (NIED) waveform data, Shimojo et al. (2014) revealed an immediate post-Tohoku seismicity activation in an area located about 10 km south of the Mw6.2 Northern Nagano source region. They also detected a few foreshocks close to the hypocenter of the Mw6.2 mainshock, within one hour before the occurrence of the moderate-size event. However, the physical processes that led to the occurrence of the Mw6.2 earthquake remained unclear. In this study we take advantage of the data recorded by a dense temporary seismic network operated by NIED from 2008 to 2012 to reveal with an unprecedented resolution the nucleation process that culminated with the occurrence of the Northern Nagano earthquake.

Data and Method

We use the waveform data of the NIED “Hizumi” temporary network, with station spacing of about 5 km or less in the study area. The data recorded by the permanent Hi-net stations (spacing of about 20 km) complements that of the dense regional network. We have first picked P- and S-wave arrivals of earthquakes on the continuous seismograms and use the pick data to locate the events. The earthquakes were then relocated using the tomoDD software (Zhang and Thurber, 2003) and a 3D velocity structure in the region (Sekiguchi et al., 2013). The newly located earthquakes were further used as MFT templates to search for new events within the 13-hour time interval, in the hypocentral region of the Mw6.2 earthquake.

Results and Discussion

We have detected a total of 286 earthquakes in the source region of the Mw6.2 event. The earthquakes are relatively small, with magnitudes less than 3.0, and distribute within two spatially distinct clusters: one of these clusters was located close to the hypocenter of the Mw 6.2 event (“West” area), the other about 5 km to the east (“East” area).

In the “East” the seismicity starts within one hour after the Tohoku-oki earthquake. The events occur off the Mw6.2 fault and expand with time from shallow towards deep locations. In the “West” the seismicity starts immediately after the passage of surface waves excited by a moderate earthquake in the Tohoku-oki aftershock area, which occurred 21 minutes after the Mw9.0 megathrust; the majority of these events distribute along the fault line of the Mw6.2 mainshock. The seismicity (in the “West”) that occurred in the immediate vicinity of the Mw6.2 hypocenter was activated about 3 hours before the mainshock and continued until its occurrence.

In both “West” and “East” regions the seismicity activation pattern shows correlation with the amplitude of the low-frequency waveforms observed at a nearby Hi-net seismic station. Such a correlation may indicate that dynamic stress changes caused by the aftershocks of the Tohoku-oki megathrust event effect the seismicity in both areas. The triggering “sensitivity” might be enhanced by excitation and circulation of fluids, which are abundant both within the shallow thick sediment as well as the lower crust of the Nagano basin, as revealed by high-resolution tomography

studies (Sekiguchi et al., 2013).

Keywords: the 2011 Northern Nagano earthquake, dense temporary regional network, Matched-Filter Technique, dynamic triggering, migration of pore-fluid

The 3-stage earthquake generation process observed during 3 months before the 2011 Tohoku earthquake

*Yoshiki SUE[1]

1.none

1 Introduction
Various phenomena were observed before the 2011 Tohoku earthquake. As for the broad band seismic network; F-net, its availability degraded. The 1st degradation occurred from December 22, 2010 to January 18, 2011, then 2nd one occurred from February 16 to March 2, after the part of the first degradation recovered to normal status. The main shock occurred on March 11, after the part of the second degradation returned to normal again.
Remarkable improvement of such measuring instrument as GNSS in recent years gives useful information about movement of crusts. So, seismic activities and measuring results of GNSS etc. are added to further check the degraded situation of the F-net.
2 Analysis
It seems that the period of approximately 3 months before the earthquake was consisted of 3 stages indicated below.
First stage
Period: End of December, 2010 to End of January, 2011.
Analysis: Accumulation of strain in the continental plate reached maximum limit in the Tohoku and Chubu regions. Possibly as a result of such situation, the wide area in Japan showed vibration or slip. Then the Pacific ocean plate stopped its advancement. Since such movements are on several day-basis, this slipping is the one like Creep. They occurred in the area far from the epicenter, the epicenter have not been formed at this moment.
Second stage
Period: Middle of February to early March
Analysis: As a result of the first stage, restless increase of stresses by the Pacific ocean plate can not be accepted any more. Then, small breakage was formed near the initial rupture point of the earthquake.
Third stage
Period: Several days before to the day of the main shock on March 11.
Analysis: Slipping of the continental plate started, and it reached the main shock.
Observed phenomenon:
On March 8, eastward movement was recorded by GNSS.
The Sanriku-oki earthquake (M7.3) occurred on March 9. The earthquakes with magnitude of 6 followed.
On March 11, The main shock of the Tohoku earthquake occurred.

Keywords: 2011Tohoku earthquake, F-net, GNSS

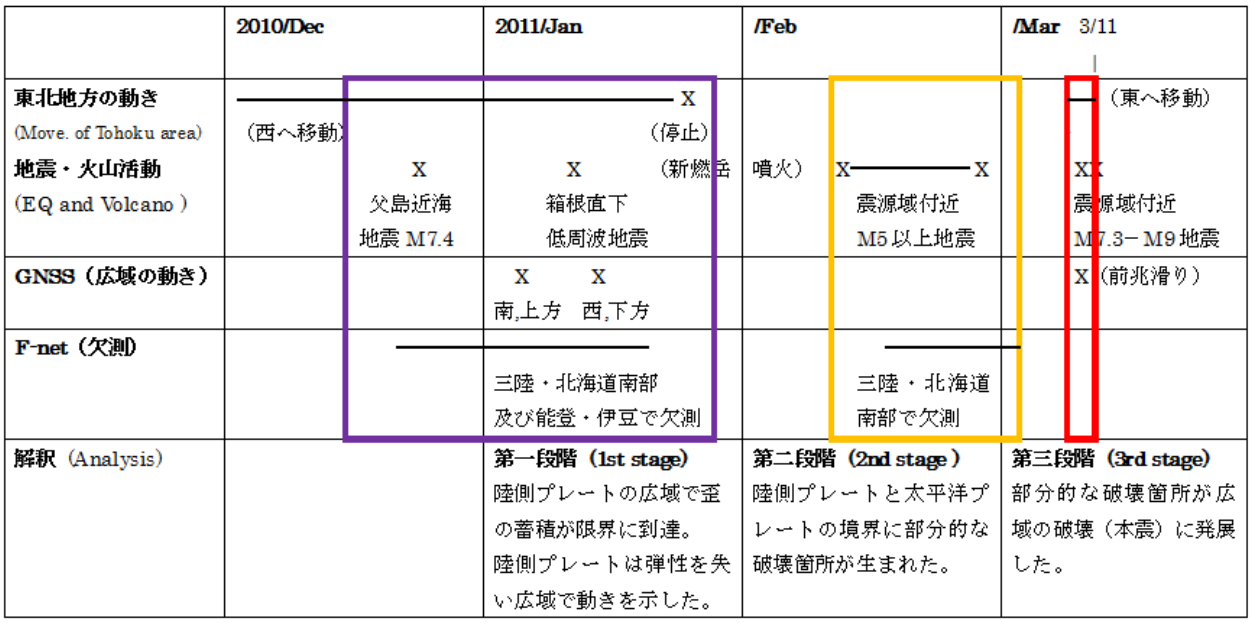

図１．2011年東北地方太平洋沖地震発生までの３段階の過程

Fig1. 3-stage process before the 2011 Tohoku earthquake

